August 27-31, 2023
FLORENCE - ITALY
ICWE 16
16th International Conference on Wind Engineering

Wind tunnel investigations on aerodynamic admittance of high-sided vehicles on a long-span bridge under crosswinds

Jiaming Zhang [1], Rong Xian [2], Cunming Ma [1,3]

[1]*Department of Bridge Engineering, Southwest Jiaotong University, Chengdu, China, zhangjiaming9406@163.com*
[2]*Guangdong Provincial Highway Construction Co., Ltd., Guangzhou, China, 4216148@qq.com*
[3]*Key Laboratory for Wind Engineering of Sichuan Province, Chengdu, China, mcm@swjtu.edu.cn*

SUMMARY:
Accurately acquiring the aerodynamic loads of vehicles on the bridge deck, including steady and unsteady components, is necessary for a precise analysis of the safety of vehicles on long-span bridges in turbulent crosswinds. However, data regarding the unsteady aerodynamic loads of vehicles are scarce, particularly when the vehicles are on a bridge deck. In this study, three different types of high-sided vehicles on a long-span bridge were tested in wind tunnels with large-scale (1:25) models for their unsteady crosswind loads, i.e., the side force admittance functions. The effects of the attack angle and vehicle position were also examined. The results show that the values of the side force admittance are kept at a constant value of slightly less than 1 when the reduced frequency is low, while the values decrease rapidly when the reduced frequency exceeds 0.1. The length of the body has a significant influence on the side force admittance function, while the vehicle position and wind angle of attack have impacts on it mainly in the low-frequency range. Furthermore, empirical expressions that accurately reflect the side force admittance functions of the three high-sided vehicles are proposed to aid engineering applications.

Keywords: aerodynamic admittance functions, high-sided vehicle, vehicle-bridge system

1. INTRODUCTION

Despite extensive research on vehicle aerodynamic characteristics (Baker, 1991; Cheli et al., 2011), most of these studies have been conducted on flat surfaces, which is not ideal for vehicles on bridge decks. However, few studies on the aerodynamic loads of vehicles on bridge decks have been conducted, particularly on unsteady aerodynamic loads. Therefore, a series of wind tunnel tests for turbulent crosswind loads of three high-sided vehicle models on a twin-box girder deck with a geometric scaling ratio of 1:25 were conducted to extend the database of unsteady aerodynamic loads of vehicles on long-span bridges in this study.

2. EXPERIMENTAL SET-UP

The experiments were undertaken in the XNJD-3 Wind Tunnel of Southwest Jiaotong University using a uniform turbulence condition with a turbulence intensity of 11.6% and a longitudinal turbulence length scale (L_u) of 25 m (at full scale). A Cobra probe (Turbulent Flow Instrumentation,

Victoria, Australia) positioned 1.5 m directly in front of the deck model was used to record the time-history of wind speeds during each test. The mean wind speed ($\bar{U}$) at the reference height corresponding to the top surface of the deck was set to 10 m/s. The aerodynamic forces of the vehicle model arranged on different lanes sequentially were measured using a high-frequency dynamic balance, and three wind attack angles of -3°, 0°, and +3° were considered. Figure 1 shows the details and dimensions of these models.

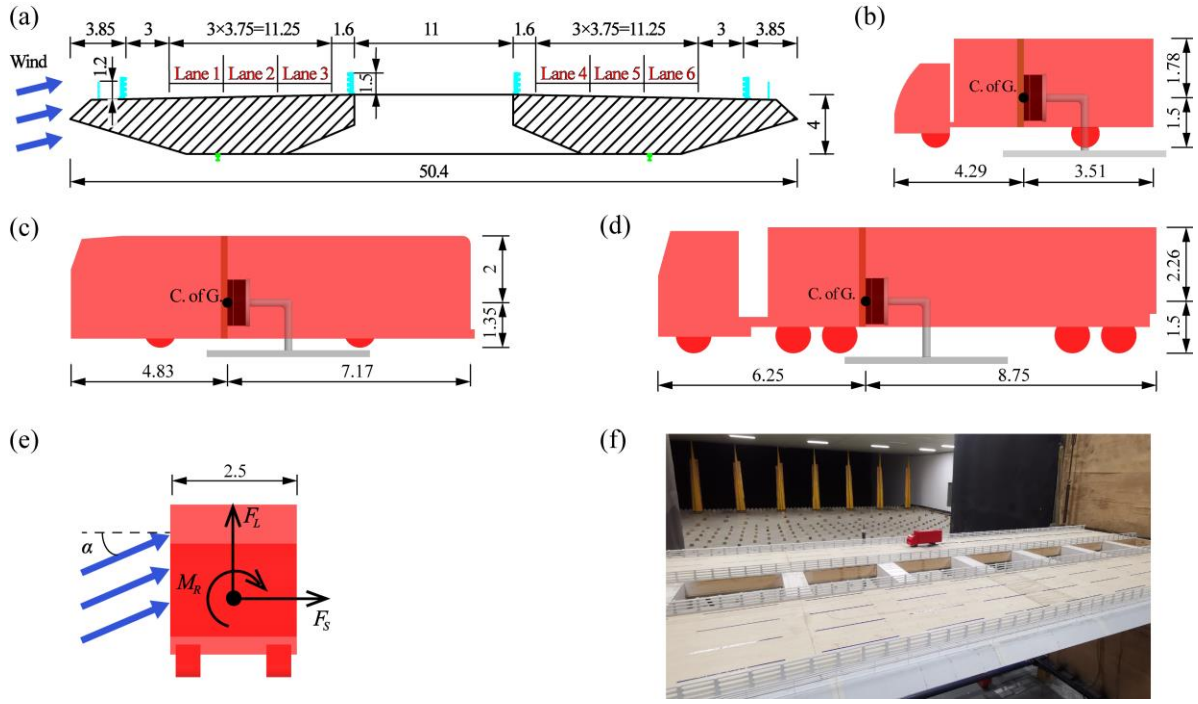

Figure 1. Dimensions of models at full scale (unit: m): (a) bridge deck; (b) medium truck; (c) bus; (d) tractor-trailer; (e) sign convention of aerodynamic forces and (f) scaled models in the wind tunnel.

3. RESULTS AND DISCUSSION

The unsteady forces acting on a vehicle are evaluated in the frequency domain by introducing the aerodynamic admittance function, which can be evaluated using the time histories of both the wind speed and the corresponding aerodynamic force, as follows (Ma et al., 2018):

$$|X_s(\bar{n})|^2 = \frac{S_S(\bar{n})}{(\rho \bar{U} A_s/2)^2\{4C_S S_u(\bar{n}) + \dot{C}_S^2 S_w(\bar{n})\}} \quad (1)$$

Where $\bar{n}$ denotes the reduced frequency $(\bar{n} = fL_u/\bar{U})$; $S_s(\bar{n})$ is the PSD of the fluctuating side force; $S_u(\bar{n})$ and $S_w(\bar{n})$ are the PSD of the longitudinal and vertical velocity components of the fluctuating wind, respectively; ρ is the air density and $\bar{U}$ is mean streamwise velocity; A_s is the side area of the vehicle model; C_S is the mean coefficient determined by the steady side force and $\dot{C}_S$ is the corresponding derivative with respect to the wind angle of attack.

The results of the side force admittance are shown in Figures 2–4 as functions of the reduced frequency ($\bar{n}$). As shown in Figure 2, the side force admittance functions for the three vehicles have similar characteristics. The amplitudes of all the three admittance functions tend to be

constant at low reduced frequencies and then decrease rapidly when the reduced frequencies exceed approximately 0.1. Furthermore, it can be inferred from comparing the admittance function amplitudes of the three vehicles that one of the key factors affecting the side force admittance function is the length of the body, i.e., the longer the length, the smaller the amplitude.

Figure 3 presents the comparison of the side force admittance of the tractor-trailer on the windward and leeward lanes at a 0° wind angle of attack. As shown in the figure, the results of vehicles on Lane 1, Lane 3, and Lane 4 are comparable and all are smaller than those on Lane 6, especially in the low frequency region. The reason for this is that the turbulence intensity of the incoming wind velocity is greatest on Lane 6 due to the interference of the bridge deck and railings.

Figure 4 illustrates the relationship between the wind angle of attack and the side force admittance function. According to Figure 4, the attack angle mainly affects the results of side force admittance in the low-frequency region, i.e., the amplitude tends to increase when the attack angle is positive, while the value tends to decrease when the attack angle is negative. The variation of side force admittance with the attack angle is not particularly significant, though, because of the narrow variation range of the angle considered in this study (only 5°). The impact of the attack angle is enhanced when the vehicle is positioned in the leeward lane, as shown in Figure 4 (b).

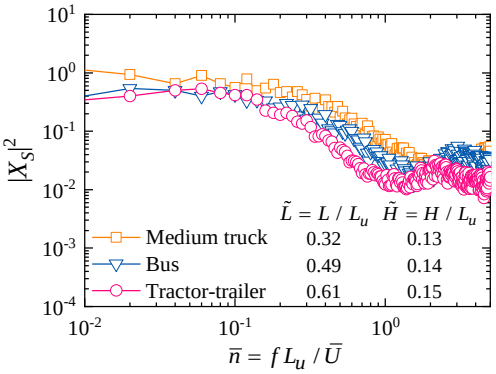

Figure 2. Side force admittance with different types of vehicles (Lane 1, 0° wind angle of attack).

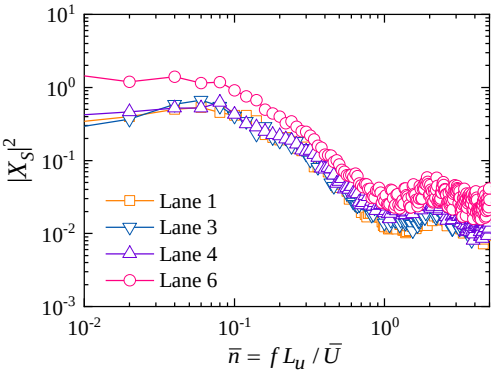

Figure 3. Side force admittance with different positions (Tractor-trailer, 0° wind angle of attack).

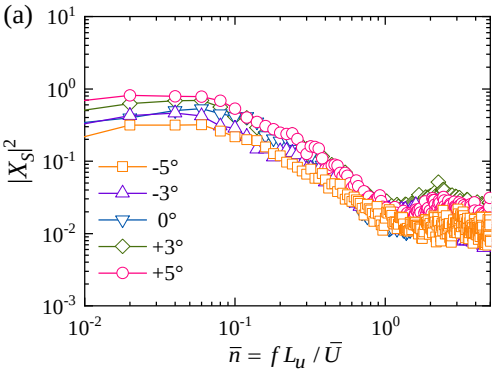

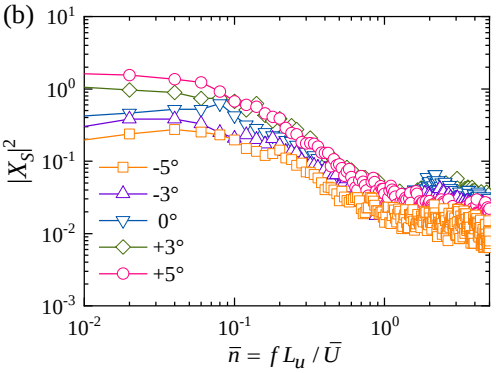

Figure 4. Side force admittance with different wind angles of attack (Tractor-trailer): (a) Lane 1 and (b) Lane4.

In addition to the comparative analysis provided here, this study also applied empirical equations

to fit the aerodynamic admittance results for road vehicles on the bridge deck. as follows:

$$|X_s(\bar{n})|^2 = \frac{a}{\left(1-\left(\frac{\bar{n}}{b}\right)\right)^4+\left(2c\frac{\bar{n}}{b}\right)^2} \quad (2)$$

Where a, b, and c represent the fitting parameters. An example of the fitting results is presented in Figure 5, where the effect of vehicle shape is specifically emphasised, and the fitting parameters are summarised in Table 1. As shown in Figure 5, the experimental data for the unsteady components of the side force can be approximated well using Eq. (2) over a nondimensional reduced frequency range of 0–1.

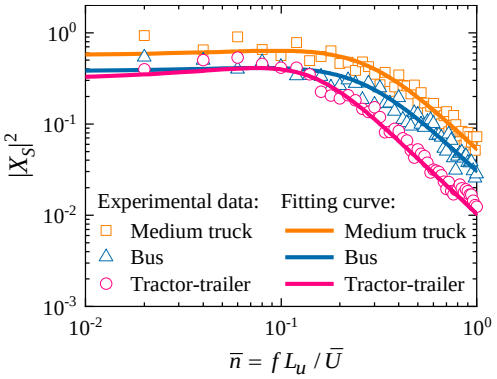

Figure 5. Fitting curves of side force admittance functions (Lane 1; 0° wind angle of attack)

Table 1. Fitted parameters

Type of vehicle	a	b	c
Medium truck	0.565	1.694	2.754
Bus	0.375	1.786	3.125
Tractor-trailer	0.309	0.601	1.635

4. CONCLUSIONS

The values of the side force admittance are kept at a constant value of slightly less than 1 when the reduced frequency is low, while the values decrease rapidly when the reduced frequency exceeds 0.1. Furthermore, the length of the body has a significant influence on the side force admittance function, while the vehicle position and wind angle of attack have impacts on it mainly in the low-frequency range. Empirical expressions that accurately reflect the side force admittance function of the high-sided vehicles on the bridge deck are proposed, which greatly facilitating engineering applications such as the refined analysis of a wind-vehicle-bridge system under turbulent winds.

ACKNOWLEDGEMENTS

The authors are grateful for their financial support from the National Natural Science Foundation of China (Grant number 52078438).

REFERENCES

Baker, C.J., 1991b. Ground vehicles in high cross winds part 2: unsteady aerodynamic forces. J. Fluids Struct. 5, 91-111.

Cheli, F., Ripamonti, F., Sabbioni, E., and Tomasini, G., 2011. Wind tunnel tests on heavy road vehicles: Cross wind induced loads-Part 2. Journal of Wind Engineering and Industrial Aerodynamics 99, 1011-1024.

Ma, C.M., Duan, Q.S., Li, Q.S., Chen, K.J., and Liao, H.L., 2018. Buffeting forces on static trains on a truss girder in turbulent crosswinds. Journal of Bridge Engineering 23, 04018086.